## Stabilization of a two-dimensional quantum electron solid in perpendicular magnetic fields

M. Yu. Melnikov, D. G. Smirnov, and A. A. Shashkin Institute of Solid State Physics, Chernogolovka, Moscow District 142432, Russia

S.-H. Huang and C. W. Liu

Department of Electrical Engineering and Graduate Institute of Electronics Engineering, National Taiwan University, Taipei 106, Taiwan

S. V. Kravchenko

Physics Department, Northeastern University, Boston, MA 02115, USA

We find that the double-threshold voltage-current characteristics in the insulating regime in the ultra-clean two-valley two-dimensional electron system in SiGe/Si/SiGe quantum wells are promoted by perpendicular magnetic fields, persisting to an order of magnitude lower voltages and considerably higher electron densities compared to the zero-field case. This observation indicates the perpendicular-magnetic-field stabilization of the quantum electron solid.

PACS numbers: 71.30.+h,73.40.Qv,71.18.+y

The ground state of a two-dimensional (2D) electron or hole system in the strongly interacting limit at low carrier densities has been predicted to be a Wigner crystal [1]. According to numerical calculations, the crystallization is expected when the interaction parameter given by the ratio of the Coulomb and Fermi energies,  $r_{\rm s} = g_{\rm v}/(\pi n_{\rm s})^{1/2} a_{\rm B}$ , exceeds about 35 [2] (here  $g_{\rm v}=2$  is the valley degeneracy,  $n_{\rm s}$  is the areal density of electrons, and  $a_{\rm B}$  is the effective Bohr radius in semiconductor). It has been theoretically predicted (see, e.g., Refs. [3–6]) that the application of a magnetic field perpendicular to the 2D plane should aid in the formation of the crystalline state. This happens because a perpendicular magnetic field decreases the amplitude of the zero-point vibrations of the carriers at the lattice sites, thereby ensuring the lattice stability. In particular, the Wigner crystal was predicted to form in a single-valley 2D electron system at Landau filling factors below approximately 0.15 [7, 8]. The presence of a residual disorder is expected to lead to an increase in the electron density of the crystallization, at least in zero magnetic field (see, e.g., Ref. [9]). There have been claims of the observation of a magneticallyinduced Wigner crystal on semiconductor surfaces, which were based on the observation of reentrant insulating phases and single-threshold current-voltage (I-V) characteristics in the insulating phases around the integer and fractional quantum Hall states (see, e.g., Refs. [10– 19), attributed to the depinning of the Wigner crystal. However, alternative mundane interpretations of the data were discussed, such as Efros-Shklovskii variable range hopping in strong electric fields [20] or percolation [21– 23].

Recently, two-threshold V-I characteristics that reveal the signature of a quantum Wigner solid and exclude mundane interpretations in terms of percolation or overheating have been observed in high-mobility silicon metal-oxide-semiconductor field-effect transistors

[24] and SiGe/Si/SiGe quantum wells [25] in a zero magnetic field. The V-I characteristics are strikingly similar to those observed for the collective depinning of the vortex lattice in type-II superconductors [26] with the voltage and current axes interchanged. The results can be described by a phenomenological theory of the collective depinning of elastic structures, which corresponds to the thermally activated transport accompanied by a peak of generated broadband current noise between the dynamic and static thresholds; the solid slides with friction as a whole over a pinning barrier above the static threshold.

In this paper, we find that perpendicular magnetic fields promote the double-threshold V-I characteristics in the insulating regime in the ultra-clean two-valley two-dimensional electron system in SiGe/Si/SiGe quantum wells. The double-threshold behavior arises at an order of magnitude lower voltages and considerably higher electron densities compared to the zero-field case so that the corresponding filling factor at high magnetic fields is equal to  $\nu \approx 0.27$ . This observation indicates the perpendicular-magnetic-field stabilization of the quantum electron solid, which is consistent with theoretical predictions.

Data obtained on ultra-high mobility were SiGe/Si/SiGe quantum wells similar to those described in Refs. [27–29]. The low-temperature electron mobility in these samples reaches  $\approx 200 \text{ m}^2/\text{Vs}$ . The approximately 15 nm wide silicon (001) quantum well is sandwiched between  $Si_{0.8}Ge_{0.2}$  potential barriers. The samples were patterned in Hall-bar shapes with the distance between the potential probes of 100  $\mu$ m and width of 50  $\mu$ m using photo-lithography. The tripletop-gate design included the main Hall-bar gate, the contact gate, and the depleting gate, separated by SiO as an insulator; this dramatically reduced the contact resistances and suppressed the shunting channel between the contacts outside the Hall bar, which manifested itself at the lowest electron densities in the insulating regime (for more details, see Ref. [29]). No additional doping was used, and the electron density was controlled by applying a positive dc voltage to the gate relative to the contacts. Measurements were conducted in an Oxford TLM-400 dilution refrigerator equipped with a magnet. The voltage was applied between the source and the nearest potential probe over a distance of 25  $\mu$ m. The current was measured by a current-voltage converter connected to a digital voltmeter. The voltage-current curves displayed slight asymmetry upon reversal of the voltage. We plotted the negative part versus the absolute voltage value for ease of representation. The electron density was determined by analyzing Shubnikov-de Haas oscillations in the metallic regime using a standard four-terminal lock-in technique. We applied saturating infrared illumination for several minutes to the samples, after which the quality of contacts enhanced and the electron mobility increased, as had been found empirically [27, 28]. The contact resistances measured below 10 kOhm. Experiments were conducted on three samples, and the obtained results were similar.

In Fig. 1 (a), we show a set of voltage-current characteristics at a temperature of 60 mK in zero magnetic field at different electron densities in the insulating regime  $n_{\rm s} < n_{\rm c}$  (here  $n_{\rm c} \approx 0.7 \times 10^{10}~{\rm cm}^{-2}$  is the critical density for the metal-insulator transition in our samples); the corresponding interaction parameter  $r_{\rm s}$  exceeds 20 at these values of  $n_{\rm s}$ . Two-threshold voltage-current curves are observed at electron densities below  $n_{\rm onset} \approx 0.3 \times 10^{10}~{\rm cm}^{-2}$ . With increasing applied voltage, the current stays near zero up to the first threshold voltage. Then, the current increases sharply until the second threshold voltage is reached, above which the slope of the V-I curves is significantly reduced, and the behavior becomes linear although not ohmic, consistent with the previously obtained results [24, 25].

The main result of the paper that the double-threshold voltage-current characteristics are promoted by perpendicular magnetic fields, B, is shown in Fig. 1 (b) at a temperature T=60 mK for B=3 T. One can see from the figure that the double-threshold behavior arises at an order of magnitude lower voltages and considerably higher electron densities compared to the zero-field case.

A phenomenological theory of the collective depinning of elastic structures was adapted for an electron solid in Ref. [24]. As the applied voltage increases, the depinning of the electron solid is indicated by the appearance of a current. Between the dynamic  $(V_d)$  and static  $(V_s)$  thresholds, the collective pinning of the electron solid occurs, and the transport is thermally activated:  $I = \sigma_0 (V - V_d) \exp[-U_c(1 - V/V_s)/k_BT]$ , where  $U_c$  is the maximal activation energy of the pinning centers,  $\sigma_0$  is a coefficient, and  $V_d$  corresponds to the pinning force. When the voltage exceeds the static threshold, the electron solid slides with friction over a pinning barrier, as determined by the balance of the electric, pinning, and friction forces, resulting in linear V-I characteris-

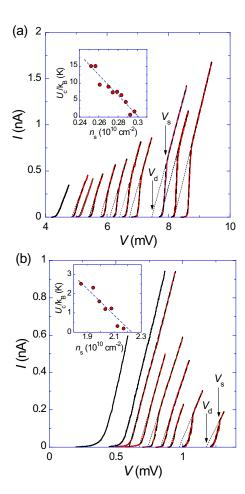


FIG. 1: (a) Voltage-current characteristics in zero magnetic field at  $T=60~\rm mK$  at electron densities (in units of  $10^{10}~\rm cm^{-2}$ , left to right): 0.306, 0.297, 0.293, 0.288, 0.284, 0.279, 0.275, 0.270, 0.261, 0.257, 0.252. (b) Voltage-current characteristics in  $B=3~\rm T$  at  $T=60~\rm mK$  at electron densities (in units of  $10^{10}~\rm cm^{-2}$ , left to right): 2.30, 2.21, 2.17, 2.12, 2.08, 2.03, 1.99, 1.94, 1.85. Also shown are the dynamic threshold  $V_{\rm d}$  obtained by the extrapolation (dotted line) of the linear part of the V-I curves to zero current and the static threshold  $V_{\rm s}$ . The dashed lines are fits to the data, see text. Insets: activation energy  $U_{\rm c}$  as a function of the electron density. The dashed line is a linear fit.

tics:  $I = \sigma_0 \, (V - V_{\rm d})$ . The corresponding fits, shown by the dashed lines in Fig. 1 (a, b), describe well the experimental two-threshold V-I characteristics in the absence or presence of a magnetic field. The activation energy  $U_{\rm c}$  obtained from the fits is plotted as a function of the electron density in the insets to Fig. 1 (a, b). The electron density, obtained by a linear extrapolation of the  $U_{\rm c}(n_{\rm s})$  dependence to zero, corresponds to  $n_{\rm onset}$  for the onset of the two-threshold V-I curves at the lowest temperatures.

In Fig. 2 (a), we plot the voltage  $V_{\rm onset}$ , determined by the linear extrapolation to zero current of the V-Icurve at the onset of the double-threshold behavior at T=30 mK, as a function of the magnetic field. The value  $V_{\rm onset}$  drops by an order of magnitude with increas-

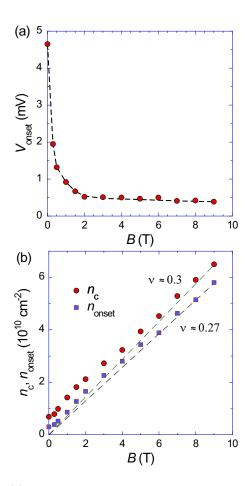


FIG. 2: (a) The onset voltage  $V_{\rm onset}$  for the double-threshold V-I curves as a function of the magnetic field at T=30 mK. The dashed line is a guide to the eye. (b) The electron density  $n_{\rm onset}$  for the onset of the double-threshold V-I curves at T=30 mK as a function of the magnetic field (squares). Also shown is the critical density  $n_c$  for the metal-insulator transition versus magnetic field (circles). The dashed lines indicate the slopes of the dependences at high B.

ing magnetic field up to  $B \approx 2$  T. In higher magnetic fields, this continues to decrease with increasing B at much slower rate.

In Fig. 2 (b), we plot the electron density  $n_{\rm onset}$  for the onset of the double-threshold V-I curves at T=30 mK as a function of the magnetic field (squares). Also shown is the critical density  $n_{\rm c}$  for the metal-insulator transition versus magnetic field (circles), determined by vanishing nonlinearity of the V-I curves when extrapolated from the insulating phase, as described in Ref. [30]. Both values increase with the magnetic field so that for all magnetic fields,  $n_{\rm onset}$  lies below  $n_{\rm c}$ . Both dependences tend at high B to linear dependences that correspond to filling factor  $\nu=n_{\rm s}hc/eB\approx0.27$  for  $n_{\rm onset}$  and  $\nu\approx0.3$  for  $n_{\rm c}$ .

In Fig. 3, we show the V-I characteristics at B=4 T and  $n_{\rm s}=2.72\times10^{10}$  cm<sup>-2</sup> at different temperatures. The fits corresponding to the activation energy  $U_{\rm c}=1.5$  K describe the data well. Unlike the B=0 case, where the V-I curves saturate below T=60 mK [25], the V-I

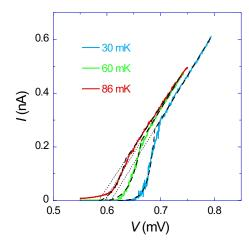


FIG. 3: Voltage-current characteristics at B=4 T and  $n_{\rm s}=2.72\times 10^{10}~{\rm cm}^{-2}$  at different temperatures. The fits corresponding to the activation energy  $U_{\rm c}=1.5$  K are shown by dashed lines.

curves in a strong magnetic field follow the expected temperature dependence down to T=30 mK, ensuring that there is no overheating down to the lowest temperatures used in our experiments.

The observed increase of the onset density  $n_{\text{onset}}$  for the double-threshold V-I curves with increasing magnetic field indicates the stabilization of the quantum electron solid in perpendicular magnetic fields. This is consistent with the theoretical prediction that the application of a perpendicular magnetic field should promote the formation of the Wigner solid by decreasing the amplitude of the zero-point vibrations of the electrons at the lattice sites [3–6]. The corresponding filling factor  $\nu \approx 0.27$  observed in our two-valley 2D electron system is in reasonable agreement with the theoretical prediction that in a disorderless single-valley 2D electron system, the Wigner crystal should form at filling factors  $\nu \lesssim 0.15$ [7, 8]. It is likely that the intermediate insulating region between  $n_{\text{onset}}(B)$  and  $n_{\text{c}}(B)$  that precedes the electron solid can be attributed to a fluctuation region. The observed drop of the onset voltage  $V_{\text{onset}}$  for the doublethreshold V-I curves with increasing magnetic field also reflects the stabilization effect of perpendicular magnetic fields. One can give a qualitative account of the behavior of  $V_{\text{onset}}$ . In zero magnetic field, the amplitude of the zero-point vibrations of the electrons at the lattice sites is relatively large, and the electron solid is easy to deform near the pinning centers. As a result, the electrons should be pinned strongly by the pinning centers, which corresponds to a relatively large onset voltage. In strong perpendicular magnetic fields, the opposite is the case. The high rigidity/uniformity of the electron solid in strong perpendicular magnetic fields may also be responsible for the observed strong temperature dependence of the V-I curves down to the lowest temperatures, unlike the B=0 case.

In summary, we have found that perpendicular mag-

netic fields promote the double-threshold V-I characteristics in the insulating regime in the ultra-clean two-valley two-dimensional electron system in SiGe/Si/SiGe quantum wells. The double-threshold behavior arises at an order of magnitude lower voltages and considerably higher electron densities compared to the zero-field case so that the corresponding filling factor at high magnetic fields is equal to  $\nu \approx 0.27$ . This observation indicates the perpendicular-magnetic-field stabilization of the quan-

tum electron solid, which is consistent with theoretical predictions. Further in-depth theoretical consideration of the effects is needed.

The ISSP group was supported by the RF State Task. The NTU group acknowledges support by the Ministry of Science and Technology, Taiwan (Project No. 112-2218-E-002-024-MBK). S.V.K. was supported by NSF Grant No. 1904024.

- [1] A. V. Chaplik, Sov. Phys. JETP 35, 395 (1972).
- [2] B. Tanatar and D. M. Ceperley, Phys. Rev. B 39, 5005 (1989).
- [3] Y. E. Lozovik and V. I. Yudson, JETP Lett. 22, 11 (1975).
- [4] F. P. Ulinich and N. A. Usov, Sov. Phys. JETP 49, 147 (1979).
- [5] H. Fukuyama, Solid State Commun. 17, 1323 (1975).
- [6] A. G. Eguiluz, A. A. Maradudin, and R. J. Elliott, Phys. Rev. B 27, 4933 (1983).
- [7] P. K. Lam and S. M. Girvin, Phys. Rev. B 30, 473 (1984).
- [8] D. Levesque, J. J. Weis, and A. H. MacDonald, Phys. Rev. B 30, 1056 (1984).
- [9] S. T. Chui and B. Tanatar, Phys. Rev. Lett. 74, 458 (1995).
- [10] E. Y. Andrei, G. Deville, D. C. Glattli, F. I. B. Williams, E. Paris, and B. Etienne, Phys. Rev. Lett. 60, 2765 (1988).
- [11] F. I. B. Williams, P. A. Wright, R. G. Clark, E. Y. Andrei, G. Deville, D. C. Glattli, C. Dorin, C. T. Foxon, and J. J. Harris, Phys. Rev. Lett. 66, 3285 (1991).
- [12] M. D'Iorio, V. M. Pudalov, and S. G. Semenchinsky, Phys. Rev. B 46, 15992 (1992).
- [13] R. L. J. Qiu, X. P. A. Gao, L. N. Pfeiffer, and K. W. West, Phys. Rev. Lett. 108, 106404 (2012).
- [14] T. Knighton, Z. Wu, V. Tarquini, J. Huang, L. N. Pfeiffer, and K. W. West, Phys. Rev. B 90, 165117 (2014).
- [15] R. Qiu, C.-W. Liu, S. Liu, and X. P. A. Gao, Appl. Sci. 8, 1909 (2018).
- [16] T. Knighton, Z. Wu, J. Huang, A. Serafin, J. S. Xia, L. N. Pfeiffer, and K. W. West, Phys. Rev. B 97, 085135 (2018).
- [17] M. S. Hossain, M. K. Ma, K. A. Villegas-Rosales, Y. J. Chung, L. N. Pfeiffer, K. W. West, K. W. Baldwin, and M. Shayegan, Phys. Rev. Lett. 129, 036601 (2022).
- [18] J. Falson, I. Sodemann, B. Skinner, D. Tabrea,

- Y. Kozuka, A. Tsukazaki, M. Kawasaki, K. von Klitzing, and J. H. Smet, Nat. Mater. 21, 311 (2022).
- [19] P. T. Madathil, K. A. V. Rosales, Y. J. Chung, K. W. West, K. W. Baldwin, L. N. Pfeiffer, L. W. Engel, and M. Shayegan, Phys. Rev. Lett. 131, 236501 (2023).
- [20] S. Marianer and B. I. Shklovskii, Phys. Rev. B 46, 13100 (1992).
- [21] H. W. Jiang, H. L. Stormer, D. C. Tsui, L. N. Pfeiffer, and K. W. West, Phys. Rev. B 44, 8107 (1991).
- [22] V. T. Dolgopolov, G. V. Kravchenko, A. A. Shashkin, and S. V. Kravchenko, Phys. Rev. B 46, 13303 (1992).
- [23] A. A. Shashkin, V. T. Dolgopolov, and G. V. Kravchenko, Phys. Rev. B 49, 14486 (1994).
- [24] P. Brussarski, S. Li, S. V. Kravchenko, A. A. Shashkin, and M. P. Sarachik, Nat. Commun. 9, 3803 (2018).
- [25] M. Y. Melnikov, A. A. Shashkin, S.-H. Huang, C. W. Liu, and S. V. Kravchenko, Phys. Rev. B 109, L041114 (2024).
- [26] G. Blatter, M. Y. Feigel'man, Y. B. Geshkenbein, A. I. Larkin, and V. M. Vinokur, Rev. Mod. Phys. 66, 1125 (1994).
- [27] M. Y. Melnikov, A. A. Shashkin, V. T. Dolgopolov, S.-H. Huang, C. W. Liu, and S. V. Kravchenko, Appl. Phys. Lett. 106, 092102 (2015).
- [28] M. Y. Melnikov, V. T. Dolgopolov, A. A. Shashkin, S.-H. Huang, C. W. Liu, and S. V. Kravchenko, J. Appl. Phys. 122, 224301 (2017).
- [29] M. Y. Melnikov, A. A. Shashkin, S. H. Huang, C. W. Liu, and S. V. Kravchenko, Triple-top-gate technique for studying the strongly-interacting 2D electron systems in heterostructures (2024), arXiv:2405.18229.
- [30] M. Y. Melnikov, A. A. Shashkin, V. T. Dolgopolov, A. Y. X. Zhu, S. V. Kravchenko, S.-H. Huang, and C. W. Liu, Phys. Rev. B 99, 081106(R) (2019).